

Effect of Continuous Micro Reinforcement and Processing Parameters on the Low-Velocity Impact Behaviour of Polymer Composite Materials

RALUCA MAIER^{1*}, ANDREI MANDOC¹, ALEXANDRU PARASCHIV¹, MARCEL ISTRATE²

¹Romanian Research Institute for Gas Turbines COMOTI, 220D Iuliu Maniu Av., 061126, Bucharest, Romania

²S.C. STIMPEX S.A., 46-48 Nicolae Teclu Str., 032368, Bucharest, Romania

Low velocity impact tests were conducted on quasi-isotropic $[\pm 45/0/90]_x$ laminates under drop weight impact from 0.7m, corresponding to a 30J energy. In this respect modified epoxy blends reinforced with carbon and Kevlar woven fabrics laminates were developed using autoclave technology. The four configurations developed for low velocity impact tests aimed at investigating several aspects like: the effect of fiber type, stacking sequence and mainly technological processing parameters, on the impact performances. The recorded Load-Time curves were plotted and visual inspection, high resolution laser scanner were used to observe the fracture characteristics of the impacted composite laminates. The results obtained showed that for tested configurations, both stacking sequence and processing parameters directly linked to fiber volume fraction, have a strong effect on the impact performances. The amount of absorbed energy, ductility index was calculated for each configuration under study. The results obtained showed that hybrid configuration exhibits lower stiffness and damage initiation energy amount when compared to carbon reinforced configurations. Nevertheless, their damage propagation energy amount and ductility index was the uppermost. This behaviour was already reported previously [1] and is partially attributed to the higher elastic energy absorption of carbon fibers that delays the propagation of delamination, and fiber breakage. Lower tenacity obtained on hybrid laminates was attributed to both lack of resin local rinse saturate and to the intrinsic anisotropy of para-aramid fibers.

Keywords: low-velocity impact, polymer matrix composites, microstructure, Fibers, Ductility Index.

Given their valuable characteristics of light weight, high strength, stiffness and high temperature resistance [2-5], fibre reinforced composites represent key materials for a wide range of engineering applications in areas like aerospace and defence. The polymeric matrix composites under study in the present work, combine the beneficial properties of both polymer resins (ability to absorb and mitigate kinetic energy) and high performance fibers (high to ultrahigh elastic modulus and strength), possess higher specific strengths than their metal counterparts, and are capable of providing equivalent impact protection at reduced weights. Despite these advantages that are revealed through their properties, fiber composites have, nevertheless, a unique interaction with the externally applied load, since severe internal damage can be generated without any external sign. Thus, low-velocity impacts pose important safety issues when it comes to structural integrity as they are capable of producing extensive damage. The most common types of damage mechanisms are delamination and matrix cracking, which are hard to hook during visual inspections, but also fiber breakage and fiber-matrix interface rupture [6,7]. Stinchcomb, et al. [8] have indicated that the mode and extent of damage in multidirectional laminates were governed by the stress states in the constituent plies and their relationships to the respective strengths. The dimensions and boundary conditions of the laminate are important, determining its flexural stiffness, for a given material whose thickness and stacking sequence are fixed [9-11]. A detailed review of the impact mechanics and dynamics of composite structures have been made by Abrate [12-14]. Despite the experimental and analytical efforts, many questions remain to be answered. Some experimental studies on the impact behaviour of woven

fabric composites were reported [13-16] nevertheless few results were reported with respect to processing parameters effect on low velocity impact performances, therefore further studies are necessary for their effective use in structural applications. The aim of the present work is to investigate low velocity impact response of the cross-ply and angle-ply carbon/epoxy and hybrid laminates. Here, three different processing cases (using autoclave technology), two type of stacking sequences for the same size, thickness and impact energy are considered. Absorbed energy amount, ductility index (DI), damage tolerance index (DTI) were calculated for each configuration while fracture characteristics of damaged specimens were analysed and 3D measured using high resolution laser scanner,

Experimental part

Materials and methodology

Laminates fabrication was performed by means of carbon woven fabrics, 200 g/m², HSC 3K, 2x2 Twill, pre-impregnated with 42%wt. of M49 epoxy resin blend. The volume fraction of carbon fibers is approximately 65%. For configuration four, one layer of dry Bidirectional Plain Kevlar 129 fibre (High Tenacity for ballistic application) was interposed between every 3 layers of mentioned CFRP pre-impregnated layers. For all laminates curing process, autoclave technology was used. The different processing parameters are summarized in table 1 below. Two stacking sequences were adopted: $[\pm 45/\pm 90]_5s$ and respectively for configuration four: $[3CFRP/1dryK [0/90]]_5s$. The panel size was 150x100 mm with nominal thickness 5 mm (according to ASTM D7136 / D7136M - 07).

* email: raluca.maier@comoti.ro, Phone: +40726943114

Table 1
CONFIGURATIONS, STACKING SEQUENCES, PROCESSING PARAMETERS

Config.	Structure Materials	Autoclave Technological Parameters	
1	CFRP [±45°/±90°]5s	T [130 °C]; P [0.7MPa]	90min. Isothermic process; heating/cooling 3 °C/min.; vacuum -0.09MPa
2		T [130 °C]; P [1.8MPa]	
3		T [120 °C]; P [0.5MPa]	120min. Isothermic process; heating/cooling 3 °C/min.; vacuum -0.09MPa
4	[3CFRP/ 1dryK [0/90]]5s	T [130 °C]; P [1.8MPa]	90min. Isothermic process; heating/cooling 3 °C/min.; vacuum -0.09MPa

Drop Weight Impact Testing and evaluation methods

Instron 9250 HV Dynatup drop tower impact testing machine was used to conduct the impact test. The test was performed by dropping a 15.5 mm diameter hemispherical striker with 4.79 kg weight on the specimens from 0.7m height. Impact velocity ranged between 3.7 and 4 m/s. The impact energy was calculated according to eq.1, corresponding to 33.5J.

$$E = C_E h \tag{1}$$

where E [J] is the potential energy of impactor prior to drop; C_E is the specified ratio of impact energy to specimen thickness, 6.7J/mm; h [mm] is the nominal thickness of specimen.

Tests were performed according to ASTM D7136 / D7136M - 07 Standard Test Method for Measuring the Damage Resistance of a Fiber-Reinforced Polymer Matrix Composite to a Drop-Weight Impact Event. As mentioned above, samples were cut to 150x100x5±0.25mm size thus no thickness effect was under study, only fiber reinforcement type, laminates architecture and stacking sequence were investigated. The microstructure of the fabricated composites was analysed by optical microscopy and scanning electron microscopy using a FEI Inspect F50. Morphology observations were aimed to investigate both structural defects (e.g. voids) as well as reinforcement network fiber distribution prior to impact tests. Visual inspection and LC15Dx CMM automatic laser scanner, with a 1.9µm accuracy and a 22µm resolution (speed 70000 points/s, daylight and reflection filters, auto-joint interface function) were used to observe the surface damage and fracture characteristics of the composite laminates

succeeding low energy impacts. Surface shape, size of the damaged area and penetration depth were measured and analysed for each sample, with the aim of establishing a correlation between processing technological parameters, reinforcement type, stacking sequences in composite laminates, impact performances and damage mechanisms.

Results and discussions

Figure 1 shows samples of Load-Time and energy-time recorded data plotted for all composite laminates configurations tested under dynamic impact regime. A general trend, behaviour can be observed on all tested specimens. Each F[N]/t[ms] curve has an ascending section of loading, corresponding to the bending stiffness due to the resistance of the composite to impact loading, at the point when the maximum load value reaches the highest maximum load (F_m), and a descending section of unloading, a descent in force occurs as a result of the impactor bouncing off the examined material surface or damage of the material.

Among tested configurations, hybrid laminates carbon/Kevlar [3CFRP/ 1dryK [0/90]]5s are clearly the less stiffest and exhibit the lowest F_m -maximum impact load. Carbon fibre laminate configurations dominate, when compared to the four (hybrid) configuration. Nevertheless, the processing parameters influence is highly important. Configuration 2 laminate exhibits the highest F_m the main parameter participating to this high rigidity being the curing pressure related to laminate compactness (1.8MPa-see table1) when compared to configurations 1 and

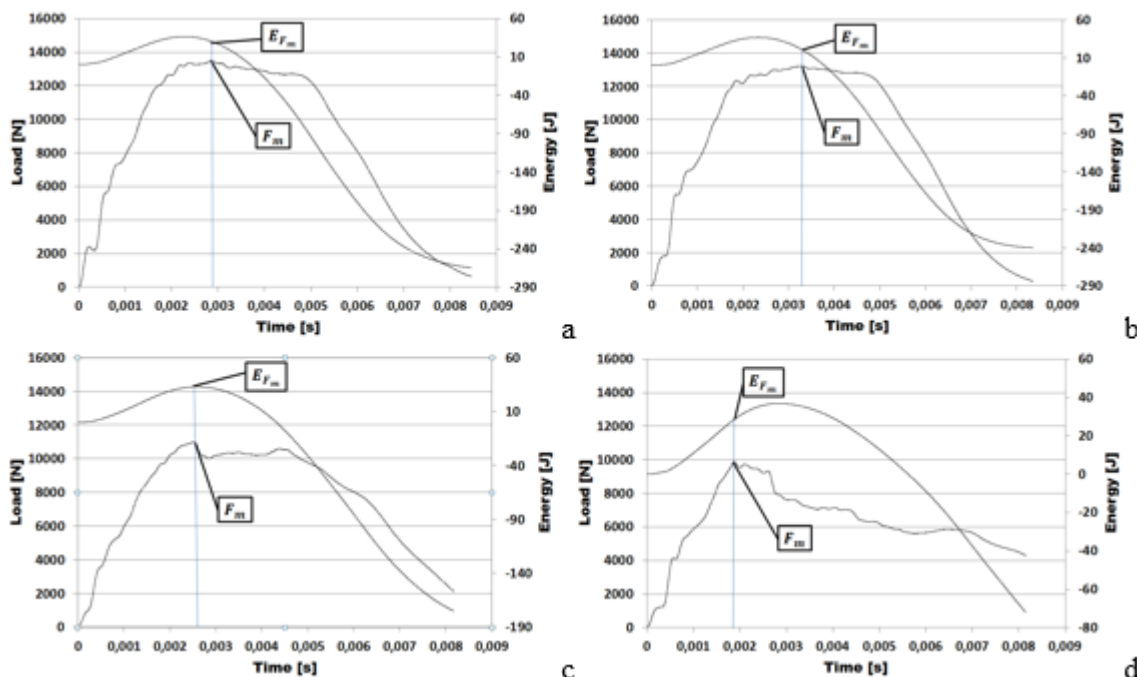


Fig. 1. Impact load/energy - time response curves obtained from the drop weight analysis, configurations (see table 1): a) 2 (CFRP-1.8 MPa); b) 1(CFRP-0.7 MPa); c) 3(CFRP-0.5 MPa); d) 4 (hybrid)

respectively 3, since laminates materials and stacking sequence are the same. An increase with 12 and respectively 20 % in stiffness was observed when comparing configuration 2 against configuration 1 and 3. Configuration four exhibits the lowest stiffness.

Micromechanics models allow the prediction of the global composite laminate stiffness based on constituent elementary structural characteristics like reinforcement type, architecture and volume fraction (eq.2).

$$C = C^m + v^f(C^f - C^m)A^f \quad (2)$$

where v^f is the fiber volume fraction, C^f is the fiber stiffness, C^m is the isotropic polymeric matrix stiffness, A^f is the deformation concentrator factor. Likewise, processing parameters related to compactness and density of the laminates (e.g. pressure applied for curing laminates) is an essential factor. The fiber volume fraction (V_f) is directly proportional with the square root of the pressure (P) as given by eq.3.

$$V_f = K1 + K2\sqrt{P} \quad (3)$$

where V_f is the fiber volume fraction, $K1, K2$ are materials constants, P is the pressure.

Furthermore, in order to investigate the fourth configuration behaviour results, microstructural analysis were performed on each configuration prior to impact testing. Morphological observations confirm the above stated theoretical aspects. Figure 2 presents the SEM images emphasizing an interspace fiber change for configuration 2 (1.8 MPa-table 1) in comparison with configuration 1 (0.7 MPa-table 1) both on warp and weft directions. The decrease in fiber network interspace for configuration 2, led to a higher compactness, superior volume fraction of the laminate and higher stiffness (see fig. 1) when compared to configuration 1.

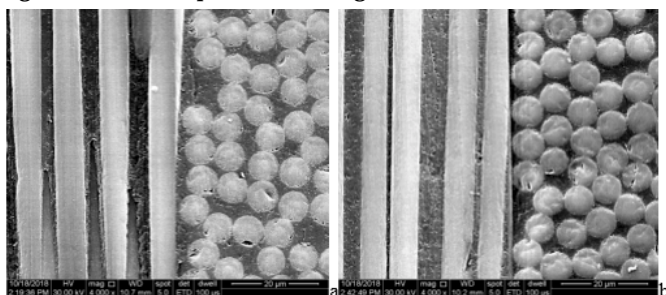


Fig. 2. SEM micrographs 4000x: a) configuration 1; b) configuration 2

The stiffest deficit observed on fourth configuration was explained following microstructural investigations, by the faulty impregnation of the Kevlar 129 network fibers by the M49 epoxy resin from the adjacent layers of pre-impregnated CFRP, in the $[3CFRP/1dryK[0/90]]_5s$ laminate architecture (fig. 3). Equally, an out of alignment of the reinforcement due in part to the deficit of the binder element (e.g. the epoxy resin) having an important role of holding the fiber network together in the predefined architecture, transferring stress between the reinforcing fibers and protecting the fibers from mechanical and environmental damage.

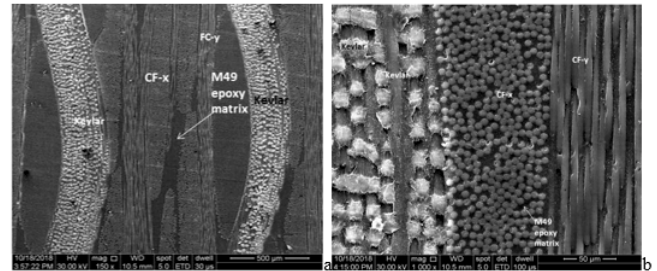


Fig. 3. SEM micrographs configuration 4: a) 150x image, out of alignment Kevlar 129 network; b) 1000x image, dry, unwetted Kevlar 129 network fibers

Furthermore, fibers diameter is not constant within the fourth hybrid laminates configuration, as it may be seen in figure 3, the average diameter of the Kevlar fibers is nearly three times higher than for the carbon fibers. Therefore, the distance between the fibers varies, being higher in the Kevlar fiber region and lesser for the smaller diameter carbon fibers region, this aspect already being analysed previously in composite laminates [18]. This aspect could be very important, because more fibers will exist on a given area the smaller the diameter of the fiber is and, thus, the interface area will be maximized, leading to a better stress distribution on the composite (as in the case of carbon composite configurations). This shall delay the initiation of defects such as matrix cracking, fibers breakage, delaminations, fact supported by the figure 1 results and table 2, where hybrid configuration four clearly exhibits lower damage initiation energy amount when compared with the other tested configurations. The main parameters used in the process of composite structure damage assessment resulting from dynamic impact within the present study are the maximum stiffness, the absorbed energy E_a and the ductility index (DI). Energy E_a is defined

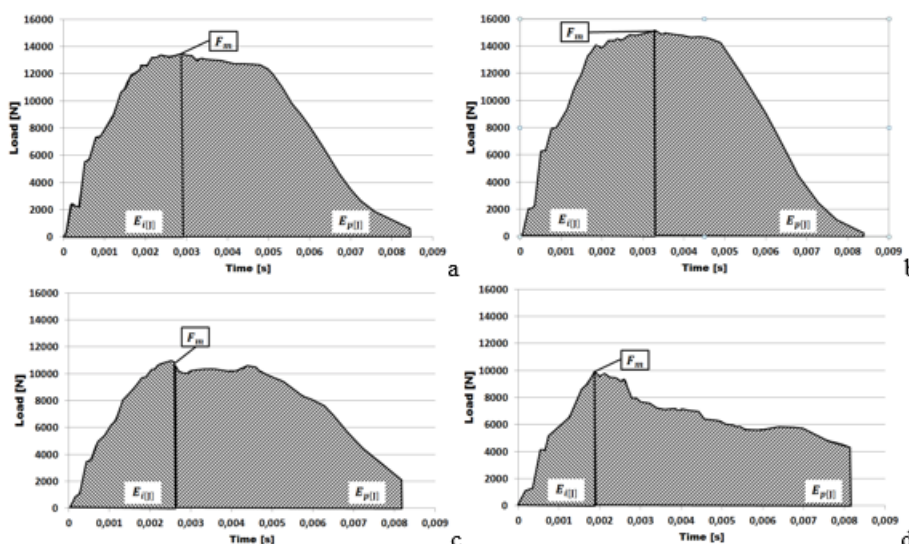


Fig. 4. Load [N]-time[s] curves showing F_{max} and absorbed energies for each tested configuration a) 2 (CFRP-1.8 MPa); b) 1 (CFRP-0.7 MPa); c) 3 (CFRP-0.5 MPa); d) 4 (hybrid)

Table 2
RESULTS OF LOW VELOCITY IMPACT TESTS FOR TESTED CONFIGURATIONS

Configuration	F_m [N]	E_i [J]	E_p [J]	E_a [J]	DI	DTI
1	13224	31	38.8	70.4	1.2	0.6
2	13466	26	46	72.6	1.7	0.8
3	10980	17	45.2	62.5	2.6	0.4
4	9894	9.8	41.4	51.2	4.2	0.2

as the amount of energy absorbed by the composite structure during dynamic impact. It is important to state that most composite materials are brittle and so can only absorb energy in elastic deformation and through damage mechanisms, and not by plastic deformation (e.g. traditional materials).

The integration of the $F[N]$ - $t[s]$ curves was performed for all tested laminate configurations in order to obtain the amount of energy absorbed E_a . The area under the load-time curve indicates absorbed energy, which corresponds to the sum of initiation energy E_i at yield point (peak force, F_m) and the energy dissipated after the yield point, damage propagation energy E_p after reaching the maximum force point. The absorbed energy E_a by the material during dynamic impact is the sum of the initiation E_i and propagation E_p energy [17]. The absorbed energy by the tested materials during dynamic impact is shown in figure 4.

Table 2 is summarizing the results for all tested configurations.

Behaviour with respect to both damage initiation and propagation mechanisms for the three CFRP configurations (1,2 and 3) are slightly different. For the second and third configurations, a critical force was emphasized F_{cr} , identifying the force for which the first relevant drop occurs. This drop is caused by a reduction of the transverse stiffness of the laminate which can be associated to a rapid propagation of delamination. The force decreases up to a rest load, F_r , after which, if the impactor retains enough energy, a reloading phase occurs up to the maximum force, F_{max} . F_{max} depends on the residual stiffness after the initial damage which takes place when the force exceeds F_{cr} . The critical impact force, F_{cr} , must be reached to trigger damage initiation. The damage stages for the small peaks observed on the force -time curves (fig. 1) at low force and energy values, corresponds to damage initiation, matrix cracks and small delamination appearance. After reaching F_{max} , damage propagation starts corresponding

to crack propagation, delamination development, fiber breaking. An exponential increase in both stiffness and initiation energy at yield point (peak force) corresponding to damage initiation, was observed for the configuration 1 to 4. Nevertheless, configurations 1 and 3 showed higher propagation energy amount when compared with the stiffest configuration 2. Configurations 1 and 2 curves (fig. 2) showed very similar behaviour, highest stiffness, highest absorbed energy and, therefore, enable a direct comparison with the two other configurations. It is worth mentioning that dry Kevlar 129 woven fibers integration within CFRP layers, in hybrid configuration four, led to significant decrease in stiffness, nevertheless the damage propagation energy is four times higher than the initiation one. Moreover, the ductility index (DI), reflecting the ductility of the material was calculated for each tested configuration, figures being presented in table 2. Likewise, figure 5 is summarizing impact results for comparison. A higher ductility index would mean that most of the total energy is expanded in crack propagation [19]. Although DI values are often associated with impact resistant materials, it should be kept in mind that a higher DI value only implies that a relatively large amount of the total impact energy is consumed through the creation and propagation of damage and does not give any information about the amount of energy absorption.

Failure was defined in this work as the partial penetration of the laminate by the indenter (fig. 6). Visual observations of the impacted samples showed that matrix and intraply cracking caused by transverse shear stresses is the trigger mechanism. Likewise, the effect of layup, stacking sequences is important, since the overall stiffness of the laminate determines the global geometry of the damaged area and that the local stacking sequence near an interface determines the shape of delamination at the interface.

Surface shape, size of the damaged area and penetration depth were measured and analysed for each sample using high accuracy LC15Dx CMM automatic laser scanner,

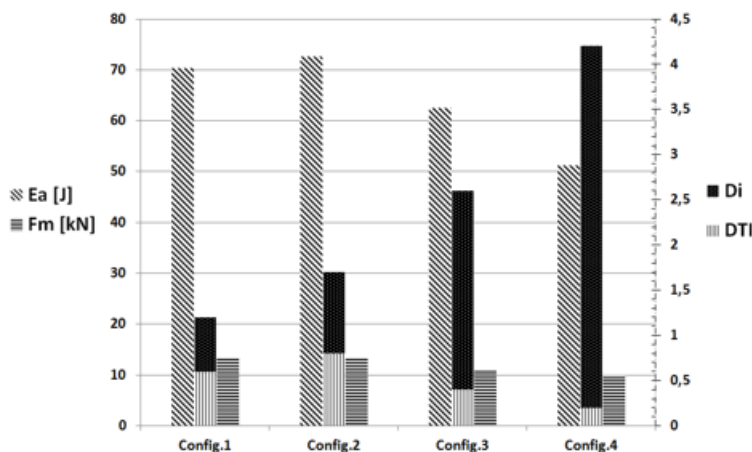


Fig. 5. Maximum force (F_m), absorbed energy (E_a), ductility index (DI), damage tolerance index (DTI) for all tested composite laminates configurations

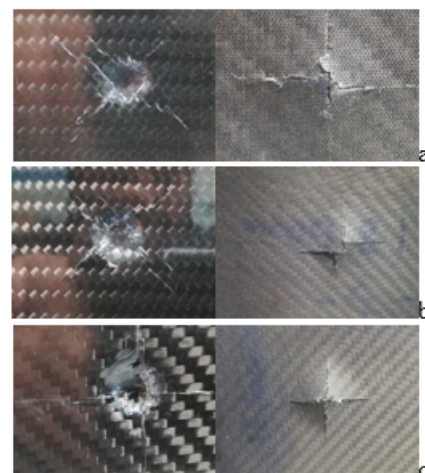
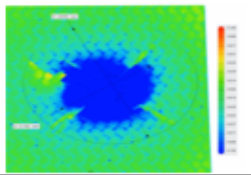
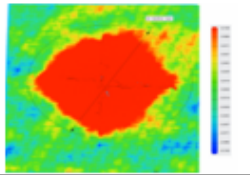

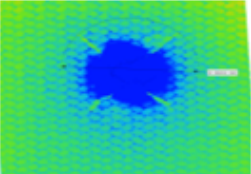
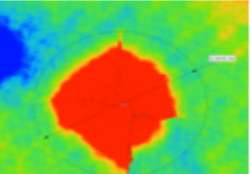

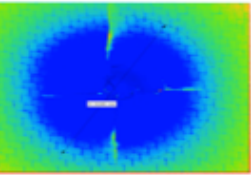
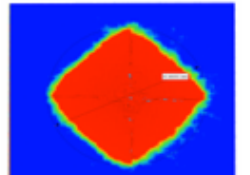



Fig. 6. Images of the damages surface areas for front and rear side of tested configurations: a) 1; b) 2; c) 4

Table 3
RESULTS OF COMPOSITE SAMPLES DAMAGE ANALYSIS (FRACTURE CHARACTERISTICS)

Config.	F_m [N]	3D measurements of post impact fractures [mm]			Damage type
		\varnothing_{front}	\varnothing_{rear}	$H_{penetration\ depth}$	
1	13224	21.8 	33.8 	2.7 	PN
2	13466	30.6 	32.7 	2.8 	PN
4	9894	50.1 	43.3 	6.7 	PN

PN-is penetration; $\varnothing_{front/rear}$ are the diameters of the damaged surface areas

results being presented in table 3. For the carbon composite, the front side has a rounded domed like aspect, indicating a homogeneous deformation. This failure type is indicative of matrix crushing, not to delamination [1]. The rear side fracture was, however, not uniform, showing preferred directions of failure. For the para-aramid composites hybrid configuration the front side looks more like diamond shape, and no damage propagation near the impact damage area as shown in table 3.

The change in the failure mechanisms between the front and the rear side modifies pattern from dome (dark area) to an elongated one (bright area). Elongated failures, following the fibers directions, are associated to the fiber-matrix interface rupture and the following delamination as already reported in the literature [20-22]. The propagation of delaminations is the dominant process and dissipates the majority of the energy. The energy required for incipient damage is matrix and interface dependent, and the peak load or energy at peak load is strongly dependent on the fiber properties. Therefore, the choice of the stacking sequence has little effect on the energy for initiation damage E_i but a large effect on the energy at peak load. These observations are in agreement with the impact results showing that for hybrid configuration peak load is lower when compared with the other configurations, a reason being the intrinsic anisotropy, low stiffness, shear strength, Young's Modulus and compressive strength, as well as the poorer adhesion to the matrix of para-aramid fibers compared to carbon fibres. Nevertheless, they exhibit significant damage propagation energy absorption as it may be seen in table 2.

Conclusions

The performance against low energy impact events of the composites tested were dominated by the intrinsic characteristics of the fiber reinforcements, the technological parameters effect related to the volumetric fraction of fibers in the composite laminates as well as the stacking sequence. Varying parameters (mainly applied

pressure) during curing process, thus modifying the volume fraction of the composites, an increase in stiffness, energy absorbed and damage tolerance index (DTI) was observed for carbon composite configurations. These later, showed the best performance due to the higher elastic energy absorption capacity of carbon fibers. Therefore, the deformation energy given to the composite by the falling weight was efficiently redistributed, delaying the initiation and propagation of defects. The performance of hybrid aramid composites was dominated by the anisotropy fibers, lack of resin local rinse saturate as well as low shear strength of these fibers. Nevertheless, for less stiffer aramid hybrid configuration, although the initiation damage energy was 40 to 70% lower than other tested configurations, a significant rise of ductility index was recorded along with an increase in damage energy propagation amount, this later being comparable with carbon composite configurations. For the carbon composite, the front side has a rounded domed like aspect, indicating a homogeneous deformation and matrix crushing failure. The rear side fracture was, however, not uniform, showing preferred directions of failure. For the para-aramid composites hybrid configuration the front side looks more like diamond shape, and no damage propagation near the impact damage area.

Acknowledgements: This work was performed within POC-A1-A1.2.3-G-2015, ID/SMIS code: P_40_422/105884, "TRANSCUMAT" Project, Grant no. 114/09.09.2016 (Subsidiary Ctr. 7/D.1.7/114/27.11.2017), supported by the Romanian Minister of Research and Innovation.

References

1. DE MORAIS, W. A., D'ALMEIDA J. R. M., GODEFROID, L. B., J. of the Braz. Soc. of Mech. Sci. & Eng., Vol. XXV, No. 4, 2003, p. 325
2. ARUN, K.V., BASAVARAJAPPA, S., SHERIGARA, B.S., Materials and Design, 31, 2010, p. 903
3. WAN, Y.Z., WANG, Y.L., HE, F., HUANG, Y., JIANG, H.J., Composites: Part A, 38, 2007, p. 495

4. HOSSEINZADEH, R., SHOKRIEH, M.M., LESSARD, L., *Compos. Sci. Technol.*, 66, 2006, p. 61
5. THANOMSIPL, C., HOGG, P.J., *Compos. Sci. Technol.*, 63, 2003, 467
6. BIBO, GA, HOGG, PJ, 1996, *J.of Mater.Science*, Vol.31, 1996, p.1115
7. ZHOU, G, *Comp. Structures*, Vol.42, 1998, p.375
8. STINCHCOMB, W.W., REIFSNIDER, K.L., YEUNG, P., MASTERS, J., *Fatigue of Fibrous Composite Materials*, ASTM STP 723, 1981, p. 64
9. ROBINSON, P, DAVIES, G.A.O., *Int. J. Impact Eng.*, 12, no.2, 1992, p.189
10. LIU, D., RAJU, BB. DANG ,X., *Int. J. Impact Eng.*, 21, no. 10, 1998, p. 837
11. CANTWELL, WJ., *Compos Sci Technol.*, 67, no. 9, 2007, p. 1900
12. ABRATE, S., *Applied Mechanics Review*, Vol. 44, no.4, 1991, p. 155
13. ABRATE, S., *Applied Mechanics Review*, Vol. 47, no.11, 1994, p. 517
14. ABRATE, S., *Compos. Struct.*, Vol. 51, 2001, p. 129
15. EBELING, T, HILTNER, A., BAER, E., FRASER, I.M., ORTON, M.L., *J. Compos. Mater.*, 1997, 31, p. 1318
16. GUILLAUD, N., FROUSTEY, C., DAU, F., VIOT, P., *Compos. Struct.*, 121, 2015, p.172
- 17.*** *Proceedings of the International Symposium On: Advanced Structural Materials*, vol.9, edited by D.S. WILKINSON, 2013, p.192
18. LANGE, F.F., RADFORD, K.C., *J.Mater.Sci.*, Vol.6, 1971, p.1197
19. RASHID, A.H.A., AHMAD, R., MUSTAPHA, M.J., *Appl. Mech. Mater.*, 271, 2014, p. 81
20. HOU, J.P., PETRINIC, N., RUIZ, C., HALLETT, S.R., *Comp.Sci.and Techol.*, Vol.60, 2000, p. 273
21. AMBUR, D.R., STARNES,,JR J.H., *J.of American Institute of Aeronautics and Astronautics*, Vol.33, 1995, p.1919
22. PARK, R., JANG, J., *J.Appl.Polym.Sci.*, Vol 75, 2000, p. 952

Manuscript received: 14.03.2019